Integrated electrical concentration and lysis of cells in a microfluidic chip

Christopher Church,[1] Junjie Zhu,[1] Guohui Huang,[2] Tzuen-Rong Tzeng,[2] and Xiangchun Xuan[1,a)]
[1]*Department of Mechanical Engineering, Clemson University, Clemson, South Carolina 29634-0921, USA*
[2]*Department of Biological Sciences, Clemson University, Clemson, South Carolina 29634-0314, USA*

(Received 7 August 2010; accepted 13 September 2010; published online 1 October 2010)

Lysing cells is an important step in the analysis of intracellular contents. Concentrating cells is often required in order to acquire adequate cells for lysis. This work presents an integrated concentration and lysis of mammalian cells in a constriction microchannel using dc-biased ac electric fields. By adjusting the dc component, the electrokinetic cell motion can be precisely controlled, leading to an easy switch between concentration and lysis of red blood cells in the channel constriction. These two operations are also used in conjunction to demonstrate a continuous concentration and separation of leukemia cells from red blood cells in the same microchannel. The observed cell behaviors agree reasonably with the simulation results. © *2010 American Institute of Physics.* [doi:10.1063/1.3496358]

I. INTRODUCTION

Cell lysis is an important step prior to the analysis of intracellular contents. To date, several methods have been demonstrated to lyse cells in microfluidic devices.[1,2] Chemical lysis uses lytic agents such as sodium dodecyl sulfate to dissolve the cell membrane or react with the membrane lipids.[3–5] Mechanical lysis uses nanoscale filtrations,[6] spherical particles,[7] or microscale sonication[8] to break down cells with shear and/or frictional forces. Thermal lysis disrupts cells at high temperatures.[9–11] Electrical lysis is based on electroporation and has been performed using either an electrical pulse[12–16] or a continuous dc electric field.[17–22]

However, the analysis of intracellular contents such as proteins normally has to be conducted based on a large number of cells. Therefore, it is often necessary to preconcentrate cells prior to lysis.[21,23] Cell trapping and concentration in microfluidic devices may take place in a contact or contactless manner. In the former case, cells have been immobilized onto a surface by chemical,[24] hydrodynamic,[25] or microelectrode-based dielectrophoretic trapping.[23,26–28] For contactless trapping, various force fields have been utilized to concentrate cells in a suspension such as acoustic,[29,30] electric,[31,32] magnetic,[33] or optical[34] forces. Additionally, insulator-based dielectrophoresis (DEP) has been recently demonstrated to continuously concentrate cells in front of posts, ridges, or droplets inside a microchannel.[35–43]

This work demonstrates an integrated concentration and lysis of mammalian cells in a constriction microchannel using dc-biased ac electric fields. Cell lysis is caused by a locally amplified electric field in the constriction, and cell concentration is achieved by the dielectrophoretic trapping in front of the constriction. With the application of dc-biased ac electric fields, the switching between cell concentration and cell lysis is easily achieved by simply adjusting the dc component.

a)Author to whom correspondence should be addressed. Electronic mail: xcxuan@clemson.edu. Tel.: 864-656-5630. FAX: 864-656-7299.

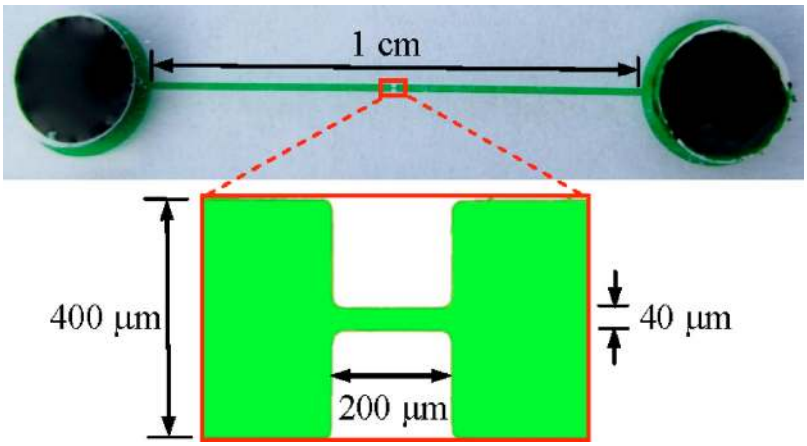

FIG. 1. Picture of the microfluidic chip and dimensions of the constriction microchannel.

These two operations are also combined to implement a continuous separation of cells. Additionally, a numerical model is developed to simulate the electrokinetic cell motion in the microchannel.

II. EXPERIMENT

A. Microchannel fabrication

The microfluidic chip was fabricated using the standard soft lithography technique.[44] Briefly, SU-8 photoresist (MicroChem Corp, Newton, MA) was first dispensed onto a clean glass slide by spin-coating (Laurell Technologies, North Wales, PA) in order to achieve a nominal thickness of 15 μm. Next, the slide was soft-baked on hot plates (HP30A, Torrey Pines Scientific, San Marcos, CA) before the photoresist film was exposed to near UV light (ABM, Inc., San Jose, CA) through a negative photomask. The photoresist was then subjected to a two-step hard bake on hot plates. After that, SU-8 developer was used to remove the photoresist that had not been treated by UV exposure, leaving a positive replica of the microchannel on the glass slide. This slide was then rinsed with isopropyl alcohol and dried with nitrogen gas. Subsequently, liquid polydimethylsiloxane (PDMS) (SYLGART 184 Silicone Elastomer Base and Curing Agent with a 10:1 weight ratio, DOW Corning Corporation, Midland, MI) was poured over the channel mold, which was then degassed in a vacuum oven (13–262–280A, Fisher Scientific, Fair Lawn, NJ) and cured in a gravity convection oven (13–246–506GA, Fisher Scientific, Fair Lawn, NJ). Last, the cured PDMS was irreversibly bonded to a clean glass slide through air plasma treating (PDC-32G, Harrick Scientific, Ossining, NY).

The microfluidic chip fabricated for the experiment consists of a straight microchannel connecting two wells with a constriction in the middle. Figure 1 shows a picture of this chip where the inset is the zoom-in view of the constriction with dimensions indicated. Specifically, the channel length is 1 cm between the two wells with a width of 400 μm. The width and length of the constriction are 40 and 200 μm, respectively. The radii of corners in the constriction are all 20 μm, and the depth of the channel is uniform at 15 μm.

B. Cell preparation

Red blood cells and leukemia cells were used in the experiments. In preparing the blood cells, a sample of sheep blood was centrifuged, resuspended in RPMI 1640 (Invitrogen, Carlsbad, CA) and stored in a refrigerator until used. Prior to experiments, the cells were centrifuge-washed three times and suspended in $1\times$ phosphate buffered saline (PBS, Fisher Scientific). The sample was then diluted 400 times before being introduced to the microchannel. K652 Leukemia cells (chronic myelogenous leukemia) were also centrifuged and suspended in RPMI 1640. These cells were

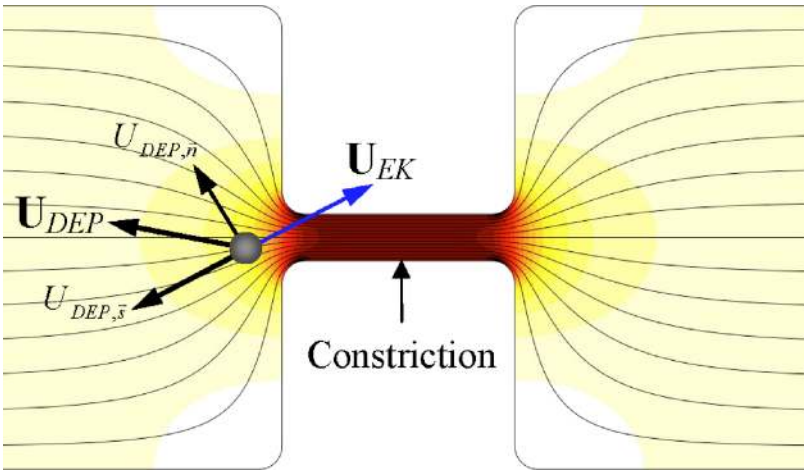

FIG. 2. Cell velocity analysis in front of a microchannel constriction, where $\mathbf{U}_{EK}$ and $\mathbf{U}_{DEP}$ are the electrokinetic and dielectrophoretic velocities, respectively. $U_{DEP,s}$ and $U_{DEP,n}$ represent the dielectrophoretic velocity components tangential and normal to a streamline, respectively. The background shows the electric field contour (the darker the higher) and the electric field lines around the constriction region in the absence of cells.

prepared at a concentration of 8.75×10^5 cells/ml and were stored at room temperature. Prior to use, the cells were washed three times and resuspended in $1\times$PBS. No further dilution was necessary before the cells were introduced to the microchannel.

C. Experimental technique

The electrical concentration and lysis of mammalian cells in the microchannel constriction was achieved by application of dc-biased ac electric fields. A function generator (33220A, Agilent Technologies, Santa Clara, CA) combined with a high-voltage amplifier (609E-6, Trek, Medina, NY) was used to supply the electric fields. The behavior of cells in the microchannel was visualized using an inverted microscope (Nikon Eclipse TE2000U, Nikon Instruments, Lewisville, TX), through which videos and images were recorded using a CCD camera (Nikon DS-Qi1Mc). The captured digital videos and images were processed using the Nikon imaging software (NIS-ELEMENTS AR 2.30). Pressure-driven cell motions were eliminated by carefully balancing the liquid heights in the two wells prior to every experiment.

III. THEORY

A. Operating mechanism

The electric field distribution around the constriction region in the fabricated microchannel is shown in Fig. 2. The lines indicate the electric field direction and the contour indicates the field intensity (the darker the higher). Due to the reduction in cross-sectional area, the root-mean-square (rms) electric field, **E** (a **bold** symbol denotes a vector hereafter), becomes strongly nonuniform in the constriction region. Thus, cells experience a dielectrophoretic force when they move electrokinetically toward the constriction. Using the dipole moment approximation, the time average of the induced dielectrophoretic motion, $\mathbf{U}_{DEP}$, of an isolated spherical cell is given by[45]

$$\mathbf{U}_{DEP} = \mu_{DEP}(\mathbf{E}\cdot\nabla\mathbf{E}), \tag{1}$$

$$\mu_{DEP} = \varepsilon_m d^2 f_{CM}/6\mu_m, \tag{2}$$

where μ_{DEP} is the dielectrophoretic mobility, ε_m is the permittivity of the suspending medium (i.e., $1\times$PBS), d is the cell diameter, μ_m is the medium viscosity, and $f_{CM}=(\sigma_c-\sigma_m)/(\sigma_c+2\sigma_m)$ is the Clausius–Mossotti (CM) factor with σ_c and σ_m being the electric conductivities of the cell and

medium, respectively. Note that in Eq. (2), the CM factors, f_{CM}, for dc and low frequency ac (1 kHz in this work) electric fields have been assumed to be approximately the same.[36,46]

As biological cells appear to be poorly conducting in dc and low-frequency ac fields[47] leading to $f_{CM}<0$ and $\mu_{DEP}<0$, they experience negative DEP in these fields. Therefore, $\mathbf{U}_{DEP}$ points away from the constriction and opposes the streamwise electrokinetic motion, $\mathbf{U}_{EK}$, of the incoming cells; see Fig. 2. The real cell velocity, $\mathbf{U}_c$, is the vector addition of $\mathbf{U}_{DEP}$ (due to the ac and dc fields) and $\mathbf{U}_{EK}$ (due to the dc field only),

$$\mathbf{U}_c = \mathbf{U}_{EK} + \mathbf{U}_{DEP} = \mu_{EK}\mathbf{E}_{dc} + \mu_{DEP}(\mathbf{E}\cdot\nabla\mathbf{E}), \tag{3}$$

where μ_{EK} is the electrokinetic mobility (a combination of fluid electro-osmosis and particle electrophoresis). As demonstrated previously,[48–50] it is convenient to express the cell velocity in Eq. (3) using streamline coordinates; see the velocity analysis on an assumed spherical cell in Fig. 2,

$$\mathbf{U}_c = (U_{EK} + U_{DEP,\vec{s}})\hat{\mathbf{s}} + U_{DEP,\vec{n}}\hat{\mathbf{n}} = \left(\mu_{EK}E_{dc} + \mu_{DEP}E\frac{\partial E}{\partial s}\right)\hat{\mathbf{s}} + \mu_{DEP}\frac{E^2}{\Re}\hat{\mathbf{n}}, \tag{4}$$

where $U_{EK}=|\mathbf{U}_{EK}|$ is the streamwise electrokinetic velocity, $U_{DEP,\vec{s}}$ is the dielectrophoretic velocity in the streamline direction with the unit vector $\hat{\mathbf{s}}$, $U_{DEP,\vec{n}}$ is the dielectrophoretic velocity normal to the streamline direction with the unit vector $\hat{\mathbf{n}}$, $E=E_{dc}+E_{ac}$ is the intensity of the total electric field with both dc and ac components, and $\Re$ is the radius of curvature of a streamline. Note that the electric field lines plotted in Fig. 2 are equivalent to the streamlines due to the similarity between flow and electric fields in pure electrokinetic flows.[51,52]

As cells experience negative DEP, i.e., $\mu_{DEP}<0$, $U_{DEP,\vec{s}}$ is against U_{EK} and thus slows down the cells when they approach the constriction; see Fig. 2. When the magnitude of $U_{DEP,\vec{s}}$ is everywhere smaller than U_{EK} or $|U_{DEP,\vec{s}}/U_{EK}|<1$, the electrokinetic motion moves cells through the constriction where they are subjected to a locally amplified electric field. Meanwhile, since $U_{DEP,\vec{n}}$ points toward the channel center plane, cells are displaced across streamlines and focused to a stream near the center of the constriction. If the local electric field within the constriction is high enough, cells that are exposed to this field for a sufficiently long time can be lysed during the passage. However, when the magnitude of $U_{DEP,\vec{s}}$ becomes greater than U_{EK} or $|U_{DEP,\vec{s}}/U_{EK}|\geq 1$ in an area, cells are unable to enter into the constriction and thus get trapped in this area (named as trapping zone in Fig. 6). It follows from Eq. (4) that the relative magnitude between $U_{DEP,\vec{s}}$ and U_{EK} is expressed as

$$\left|\frac{U_{DEP,\vec{s}}}{U_{EK}}\right| = \left|\frac{\mu_{DEP}E\dfrac{\partial E}{\partial s}}{\mu_{EK}E_{dc}}\right| = \frac{(1+\alpha)^2}{\alpha}\left|\frac{\mu_{DEP}}{\mu_{EK}}\frac{\partial E_{ac}}{\partial s}\right|, \tag{5}$$

where α is defined as the ratio of the dc field to the rms ac field, i.e., $E=E_{dc}+E_{ac}=E_{ac}(1+\alpha)$. Therefore, the transition between lysing and trapping cells can be realized by simply adjusting E_{dc} or equivalently α if E_{ac} is maintained. Note that the prefactor $(1+\alpha)^2/\alpha$ in Eq. (5) decreases monotonically with increasing α in the range of $0<\alpha<1$. That is to say lowering α or reducing the dc field component will allow the dielectrophoretic motion to dominate causing cells to be concentrated (i.e., $|U_{DEP,\vec{s}}/U_{EK}|\geq 1$), while increasing α allows the electrokinetic motion to dominate causing cells to be lysed (i.e., $|U_{DEP,\vec{s}}/U_{EK}|<1$).

B. Numerical modeling

A numerical model was developed in order to predict the electrical concentration and lysis of cells in the constriction microchannel. It is based on the model developed by Kang *et al.*,[53,54] where the effects of cells on the electric and flow fields are neglected. Instead, a correction factor, λ, is introduced to account for the influence of cell size, cell-cell interactions, etc. on the dielectrophoretic velocity. Thus, Eq. (3) can be revised to show the simulated cell velocity as

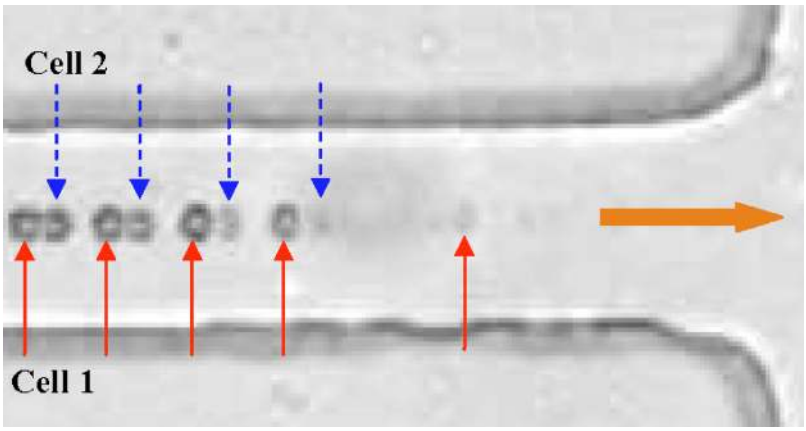

FIG. 3. Superimposed image of two red blood cells (highlighted as cell 1 and cell 2) illustrating the typical process of electrical lysis in the microchannel constriction. The block arrow indicates the flow direction in the channel.

$$\mathbf{U}_c = \mu_{EK}\mathbf{E}_{dc} + \lambda\mu_{DEP}(\mathbf{E}\cdot\nabla\mathbf{E}), \tag{6}$$

which is used as an input to the particle tracing function in COMSOL® (Burlington, MA) for computing the cell trajectory. This model has been validated in simulating the electrical manipulations of particles and cells in various microchannels.[48–50,53–57]

In conducting the simulation, a 2D model was used to calculate the electric field distribution, $\mathbf{E}=-\nabla\phi$, from the Laplace equation, $\nabla^2\phi=0$, where ϕ denotes the electric potential. This treatment has been proved to be reasonable in microchannels of a uniform depth.[48–50,53–57] The electrokinetic mobility, μ_{EK}, of red blood cells in $1\times$PBS was determined to be approximately 1.5×10^{-4} ($cm^2\ V^{-1}\ s^{-1}$) by measuring their average velocity in the region distant from the channel constriction. For the leukemia cells, the electrokinetic mobility was determined to be approximately 1.2×10^{-4} ($cm^2\ V^{-1}\ s^{-1}$). The dielectrophoretic mobility, μ_{DEP}, was calculated using Eq. (2), where the blood and leukemia cells were both assumed spherical with an average diameter of 5 μm and 8 μm, respectively. The dynamic viscosity and permittivity were assumed to be equal to those of pure water at 25 °C. The correction factor, λ, was set to 0.5 for the red blood cells and 0.3 for the leukemia cells, which are consistent with previous values for polystyrene beads with similar sizes.[48–50,53–57]

IV. RESULTS AND DISCUSSION

A. Demonstration of electrical lysis and concentration of red blood cells

Lysing and concentrating red blood cells in the constriction microchannel were first examined individually by fixing the applied total voltage (and thus the total electric field) while adjusting the ratio of the dc to ac voltage. The onset of electrical lysis was observed at an average field of 1000 V/cm in the constriction, which is consistent with other sources.[19,20,22] It follows that any field higher than this threshold value would cause cell lysis. A typical lysis process is illustrated in Fig. 3, where the two red blood cells gradually became invisible before moving out of the constriction. The total voltage was fixed at 160 V during this experiment, and the resulting 1600 V/cm average electric field in the constriction was sufficiently high to guarantee complete lysis of red blood cells. The following conditions were tested: (1) 160 V pure dc, (2) 80 V dc/80 V ac (rms value), (3) 40 V dc/120 V ac, and (4) 15 V dc/145 V ac.

In the first case of 160 V pure dc, the electrokinetic motion driving red blood cells was significantly stronger than the dielectrophoretic opposing motion at the constriction. Therefore, cells moved quickly through the constriction and were only exposed to the locally amplified electric field for a very short duration. The residence time of cells in the 200-μm long constriction region was estimated to be about 80 ms. The superimposed image from this test is shown in Fig.

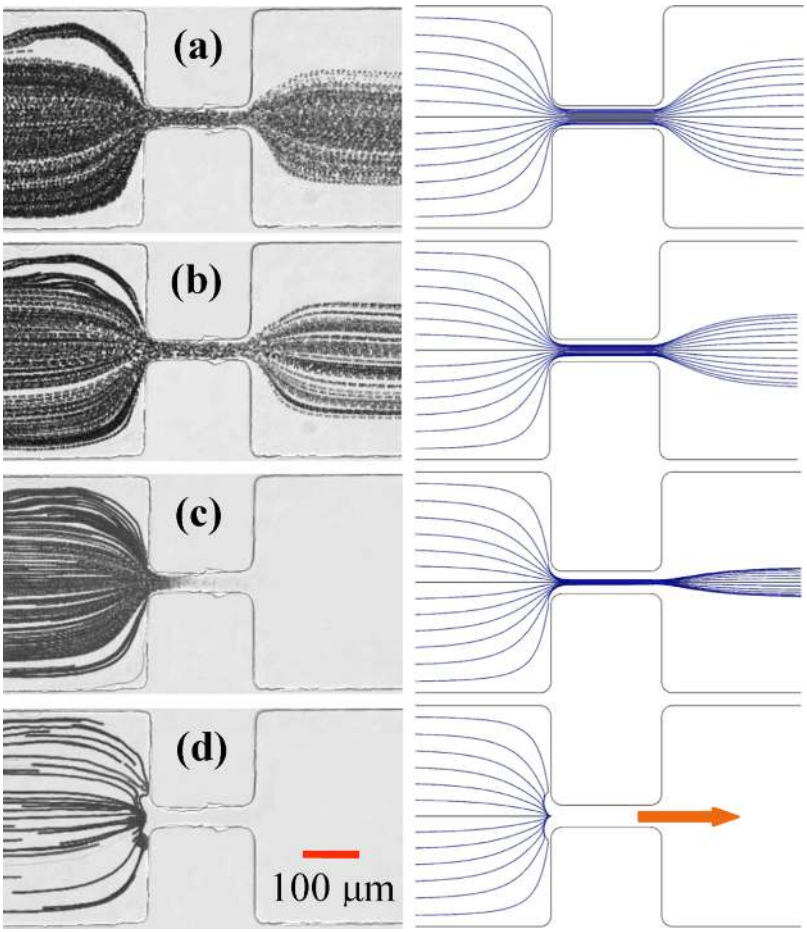

FIG. 4. Effects of the dc to ac field ratio on the electrokinetic transport of red blood cells in the microchannel constriction. The left column shows the superimposed images, and the right column shows the simulated cell trajectories for (a) 160 V pure dc, little lysis; (b) 80 V dc/80 V ac, partial lysis; (c) 40 V dc/120 V ac, complete lysis; and (d) 15 V dc/145 V ac, trapping. The block arrow indicates the flow direction in the channel.

4(a), where the cell trajectories are clearly visible past the constriction indicating that little lysis has taken place. Moreover, the cells were traveling in a narrower stream after the constriction due to the known dielectrophoretic focusing.[49] The right plot in Fig. 4(a) shows the numerically predicted cell trajectories, which agrees with the experimental result.

In the second case of 80 V dc and 80 V ac, the cell velocity resulting from electrokinetic motion was reduced by half as compared to the first case. It was, however, still stronger than that from the opposing dielectrophoretic motion. Therefore, red blood cells moved through the constriction with a twice-long exposure time to the same electric field as in the pure dc case. As seen from the superimposed image in Fig. 4(b), the cell trajectories are still visible past the constriction while with more gaps in between, indicating a higher percentage of cells being lysed than in Fig. 4(a). The right plot in Fig. 4(b) shows the simulated cell trajectories for this case, which predicts a much better focusing than the experiment. This could be due to the induced changes in the electrical properties of both the cells and the buffer (e.g., release of cellular contents into the solution) as a consequence of the cell electroporation/lysis in the constriction region.

In the third case of 40 V dc and 120 V ac, the cells could still move into the constriction while at an even slower velocity than in the second case. Consequently, all cells were lysed when they moved through the constriction as a result of the extended exposure time to the locally high

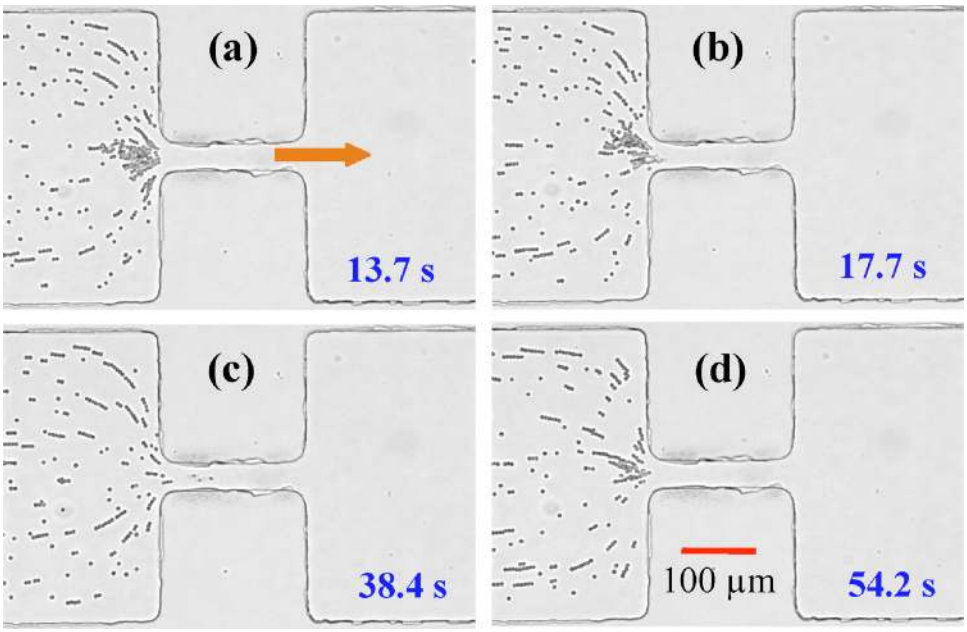

FIG. 5. Sequence of snapshot images of red blood cells demonstrating the transition from trapping at 15 V dc/145 V ac (a) to lysing at 25 V dc/145 V ac [(b) and (c)] and back to trapping 15 V dc/145 V ac (d). The time at which each snapshot was taken is displayed on each image in the sequence. The block arrow indicates the flow direction in the microchannel.

electric field. This complete cell lysis is evidenced from the superimposed image in Fig. 4(c), where the trajectories of red blood cells faded and disappeared as they moved through the constriction. As the current model in COMSOL® does not consider the cell lysis condition, the simulation result in Fig. 4(c) for this case only predicts that the cells should pass through the constriction in a well-focused manner.

In the last case of 15 V dc and 145 V ac, the electrokinetic motion was not strong enough to overcome the opposing dielectrophoretic motion, so the cells got trapped and accumulated in front of the constriction. This is evident from the superimposed image in Fig. 4(d), where there is no trace of the cells moving into the constriction. It should be noted that in this test, the cell velocity was very low (about 20 μm/s before approaching the constriction) due to the small dc field, which resulted in the fewer cells present in the image than the other cases in Fig. 4. The simulated cell trajectories in Fig. 4(d) (right plot) are consistent with the experimental observation. These above tests, as illustrated in Fig. 4, demonstrate the usefulness of dc-biased ac electric fields in cell manipulations as the cell velocity can be controlled by tuning the dc component while keeping the total voltage fixed.

B. Switching between electrical lysis and concentration of red blood cells

dc-biased ac electric fields were also demonstrated to implement the easy switching between lysis and concentration of red blood cells. This was achieved by making a small adjustment to the dc portion of the total voltage across the constriction microchannel. To this end, the ac voltage was fixed at 145 V ac (rms value). When the test began, the dc voltage was set at 15 V consistent with the trapping condition determined above. At this ratio of dc to ac field, the cells were trapped in front of the constriction as shown in Fig. 5(a). Once enough cells had accumulated, the dc voltage was increased to 25 V, causing the electrokinetic motion to overcome the opposing dielectrophoretic motion. As a consequence, the cells passed through the constriction and were lysed completely. The start of this process can be seen in Fig. 5(b), where the accumulation in front of the constriction has started to become smaller as cells have begun to move through the constriction and be lysed. As cell lysis was allowed to continue, all of the previous accumulation caused by the

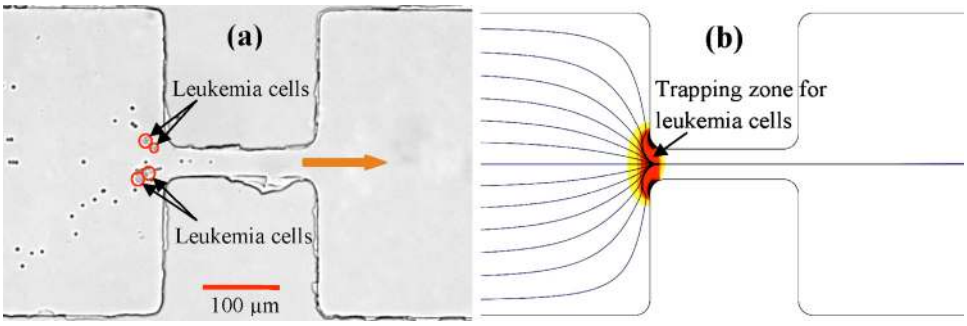

FIG. 6. Integration of electrical concentration of leukemia cells and electrical lysing of red blood cells in the microchannel constriction: (a) experimentally recorded snapshot image with the trapped leukemia cells highlighted with circles for clarity and (b) numerically predicted trapping zone for leukemia cells and trajectories for red blood cells. The block arrow indicates the flow direction.

dielectrophoretic trapping passed through the constriction and disappeared, as demonstrated in Fig. 5(c). At this point, the dc voltage was reduced back to 15 V, and the dielectrophoretic motion became once again dominant, resulting in a new trapping of cells. This can be seen in Fig. 5(d) where trapping has caused red blood cells to begin accumulating in front of the constriction once more.

C. Integrated electrical concentration and lysis of leukemia cells and red blood cells

The above demonstrated electrical techniques for concentrating and lysing cells were also integrated to implement a selective isolation of leukemia cells from red blood cells in the microchannel constriction. As the dielectrophoretic motion is proportional to the square of the cell diameter [see Eq. (2)], the larger leukemia cells should experience a stronger opposing dielectrophoretic motion than the smaller red blood cells at the same electric field. It is thus expected that there should exist an electric field with an appropriate dc to ac ratio, at which the leukemia cells can be trapped in front of the constriction while red blood cells can still move through the constriction and get lysed.

In this proof-of-principle experiment, the dc and ac voltages were set to 30 and 170 V, respectively. Figure 6(a) shows a snapshot of this process where the leukemia cells (highlighted with circles for clarity) can be seen trapped and the blood cells can be seen passing through the constriction and being lysed. This selective concentration and lysis essentially result in a continuous separation between the leukemia and red blood cells. One current issue that affects this separation at times is the interaction between the two types of cells. As leukemia cells are trapped in front of the constriction, some red blood cells may be pulled toward the trapped leukemia cells forming chains via DEP, leading to an incomplete separation. Figure 6(b) shows the numerically predicted trajectories of red blood cells (again, lysis is not simulated as explained earlier) and trapping zone for leukemia cells [i.e., the region with $|U_{\mathrm{DEP},\vec{s}}/U_{\mathrm{EK}}| \geq 1$ (Ref. 58)], which both agree with the experimental results.

If the applied electric field is not high enough, red blood cells may move through the microchannel constriction without lysis. Meanwhile, leukemia cells can still be trapped in front of the constriction if $|U_{\mathrm{DEP},\vec{s}}/U_{\mathrm{EK}}| \geq 1$, which can be achieved simply by decreasing the dc to ac field ratio, α [see Eq. (5)]. For example, the numerical modeling indicates that the use of 5 V dc and 75 V ac leads to the trapping of leukemia cells. At this condition, red blood cells may remain unlysed as the corresponding total electric field of 800 V/cm in the constriction is smaller than the threshold value mentioned earlier.

D. Joule heating effects

As the working buffer, 1 × PBS, is highly conductive and the constriction region amplifies the local electric field, the experiments were monitored for Joule heating effects. In doing so, the electric current was measured as soon as the electric field was applied and monitored every 10 s for 2 min to observe the rise over time. Under the applied 160 V across the microchannel, the current on application was about 250 μA and rose to approximately 260 μA after 1 min, where the increase after this point became minimal. Therefore, the average temperature elevation in the buffer is estimated to be about 2 °C in this experiment.[59] Such Joule heating effects can be mitigated by reducing the channel depth or lowering the buffer concentration. Note that the calculated thermal diffusion time is about 40 s over a 2-mm-thick PDMS slab.[60]

V. SUMMARY

Electrical concentration and lysis of red blood cells have been performed in a microfluidic chip with a single constriction microchannel using dc-biased ac electric fields. In these processes, the dc field drives the cell sample and controls the cell traveling speed through the channel. The ac field is mainly responsible for achieving the desired field magnitude and gradient in the constriction region for electrically lysing and dielectrophoretically trapping the cells. The ability to switch between these two processes by making only a small adjustment to the applied dc voltage without significantly changing the overall electric field has also been demonstrated. Further, both trapping and lysing have been used in conjunction to implement a selective enrichment and isolation of leukemia cells from red blood cells in the constriction microchannel. Such a continuous separation of mammalian cells is envisioned to be useful for biomedical and clinical applications.

ACKNOWLEDGMENTS

This work was partially supported by NSF under Grant No. CBET-0853873.

[1] H. Yan, B. Y. Zhang, and H. K. Wu, Electrophoresis **29**, 1775 (2008).
[2] J. Kim, M. Johnson, P. Hill, and B. K. Gale, Integrative Bio **1**, 574 (2009).
[3] P. C. H. Li and D. J. Harrison, Anal. Chem. **69**, 1564 (1997).
[4] C. Prinz, J. O. Tegenfeldt, R. H. Austin, E. C. Cox, and J. C. Sturm, Lab Chip **2**, 207 (2002).
[5] J. W. Hong, V. Studer, G. Hang, W. F. Anderson, and S. R. Quake, Nat. Biotechnol. **22**, 435 (2004).
[6] D. Di Carlo, K. H. Jeong, and L. P. Lee, Lab Chip **3**, 287 (2003).
[7] J. Kim, S. H. Jang, G. Jia, J. V. Zoval, N. A. Da Silva, and M. J. Madou, Lab Chip **4**, 516 (2004).
[8] P. Belgrader, D. Hansford, G. T. A. Kovacs, K. Vankateswaran, R. Mariella, F. Milanovich, S. Nasarabadi, M. Okuzumi, F. Pourahmadi, and M. A. Northrup, Anal. Chem. **71**, 4232 (1999).
[9] L. C. Waters, S. C. Jacobson, N. Kroutchinina, J. Khandurina, R. S. Foote, and J. M. Ramsey, Anal. Chem. **70**, 158 (1998).
[10] J. El-Ali, S. Gaudet, A. Guenther, P. K. Sorger, and K. F. Jensen, Anal. Chem. **77**, 3629 (2005).
[11] S. K. Baek, J. Min, and J. H. Park, Lab Chip **10**, 909 (2010).
[12] H. Lu, M. A. Schmidt, and K. F. Jensen, Lab Chip **5**, 23 (2005).
[13] M. Khine, A. Lau, C. Ionescu-Zanetti, J. Seo, and L. P. Lee, Lab Chip **5**, 38 (2005).
[14] K. Park, D. Akin, and R. Bashir, Biomed. Microdevices **9**, 877 (2007).
[15] P. J. Marc, C. E. Sims, M. Bachman, G. P. Li, and N. L. Allbritton, Lab Chip **8**, 710 (2008).
[16] G. Mernier, N. Piacentini, T. Braschler, N. Demierre, and P. Renaud, Lab Chip **10**, 2077 (2010).
[17] H. Y. Wang, A. K. Bhunia, and C. Lu, Biosens. Bioelectron. **22**, 582 (2006).
[18] H. Y. Wang and C. Lu, Chem. Commun. **33**, 3528 (2006).
[19] H. Y. Wang and C. Lu, Anal. Chem. **78**, 5158 (2006).
[20] D. W. Lee and Y. H. Cho, Sens. Actuators B **124**, 84 (2007).
[21] N. Bao and C. Lu, Appl. Phys. Lett. **92**, 214103 (2008).
[22] N. Bao, T. Le, J. Chen, and C. Lu, Integrative Bio **2**, 113 (2010).
[23] Q. Ramadan, V. Samper, D. Poenar, Z. Liang, C. Yu, and T. M. Lim, Sens. Actuators B **113**, 944 (2006).
[24] D. Juncker, H. Schmid, and E. Delamarche, Nature Mater. **4**, 622 (2005).
[25] A. Y. Lau, P. J. Hung, A. R. Wu, and L. P. Lee, Lab Chip **6**, 1510 (2006).
[26] G. Fuhr, T. Muller, V. Baukloh, and K. Lucas, Hum. Reprod. **13**, 136 (1998).
[27] I. F. Cheng, H. C. Chang, D. Hou, and H. C. Chang, Biomicrofluidics **1**, 021503 (2007).
[28] R. Pethig, Biomicrofluidics **4**, 022811 (2010).
[29] M. Evander, L. Johansson, T. Lilliehorn, J. Piskur, M. Lindvall, S. Johansson, M. Almqvist, T. Laurell, and J. Nilsson, Anal. Chem. **79**, 2984 (2007).
[30] L. Y. Yeo and J. R. Friend, Biomicrofluidics **3**, 012002 (2009).

[31] D. Hou, S. Maheshwari, and H. C. Chang, Biomicrofluidics **1**, 014106 (2007).
[32] J. Du, Y. Juang, J. Wu, and H. Wei, Biomicrofluidics **2**, 044103 (2008).
[33] S. H. Huh, C. Y. Kim, H. S. Jeong, and A. Nakajima, J. Appl. Phys. **101**, 104317 (2007).
[34] A. Kumar, J. S. Kwon, S. J. Williams, N. G. Green, N. K. Yip, and S. T. Wereley, Langmuir **26**, 5262 (2010).
[35] B. H. Lapizco-Encinas, B. A. Simmons, E. B. Cummings, and Y. Fintschenko, Anal. Chem. **76**, 1571 (2004).
[36] B. H. Lapizco-Encinas, B. A. Simmons, E. B. Cummings, and Y. Fintschenko, Electrophoresis **25**, 1695 (2004).
[37] B. H. Lapizco-Encinas, R. V. Davalos, B. A. Simmons, E. B. Cummings, and Y. Fintschenko, J. Microbiol. Methods **62**, 317 (2005).
[38] B. G. Hawkins, A. E. Smith, Y. A. Syed, and B. J. Kirby, Anal. Chem. **79**, 7291 (2007).
[39] P. K. Thwar, J. J. Linderman, and M. A. Burns, Electrophoresis **28**, 4572 (2007).
[40] M. D. Pysher and M. A. Hayes, Anal. Chem. **79**, 4552 (2007).
[41] P. Sabounchi, A. M. Morales, P. Ponce, L. P. Lee, B. A. Simmons, and R. V. Davalos, Biomed. Microdevices **10**, 661 (2008).
[42] H. Shafiee, J. L. Caldwell, M. B. Sano, and R. V. Davalos, Biomed. Microdevices **11**, 997 (2009).
[43] H. Shafiee, J. L. Caldwell, and R. V. Davalos, J. Assoc. Lab. Autom. **15**, 224 (2010).
[44] D. C. Duffy, J. C. McDonald, O. J. A. Schueller, and G. M. Whitesides, Anal. Chem. **70**, 4974 (1998).
[45] H. Morgan, N. G. Green, and A. C. Electrokinetic, *Colloids and Nanoparticles* (Research Studies, Hertfordshire, United Kingdom, 2002).
[46] J. Voldman, Annu. Rev. Biomed. Eng. **8**, 425 (2006).
[47] G. H. Markx, Y. Huang, X. F. Zhou, and R. Pethig, Microbiology **140**, 585 (1994).
[48] J. Zhu, T. J. Tzeng, G. Hu, and X. Xuan, Microfluid. Nanofluid. **7**, 751 (2009).
[49] J. Zhu and X. Xuan, Electrophoresis **30**, 2668 (2009).
[50] J. Zhu and X. Xuan, J. Colloid Interface Sci. **340**, 285 (2009).
[51] E. B. Cummings, S. K. Griffiths, R. H. Nilson, and P. H. Paul, Anal. Chem. **72**, 2526 (2000).
[52] J. G. Santiago, Anal. Chem. **73**, 2353 (2001).
[53] K. H. Kang, X. Xuan, Y. Kang, and D. Li, J. Appl. Phys. **99**, 064702 (2006).
[54] K. Kang, Y. Kang, X. Xuan, and D. Li, Electrophoresis **27**, 694 (2006).
[55] Y. Kang, B. Cetin, Z. Wu, and D. Li, Electrochim. Acta **54**, 1715 (2009).
[56] C. Church, J. Zhu, G. Wang, T. J. Tzeng, and X. Xuan, Biomicrofluidics **3**, 044109 (2009).
[57] C. Church, J. Zhu, J. Nieto, G. Keten, E. Ibarra, and X. Xuan, J. Micromech. Microeng. **20**, 065011 (2010).
[58] J. L. Baylon-Cardiel, B. H. Lapizco-Encinas, C. Reyes-Betanzo, A. V. Chavez-Santoscoy, and S. O. Martinez-Chapa, Lab Chip **9**, 2896 (2009).
[59] X. Xuan, Electrophoresis **29**, 33 (2008).
[60] D. Erickson, D. Sinton, and D. Li, Lab Chip **3**, 141 (2003).